Quantum Size Effect in Semimetal Bismuth Antimony Wires and Films

Albina NIKOLAEVA[1,2], Leonid KONOPKO[1,2], Vladimir GRABOV[3], Evghenii DEMIDOV[3], Natalia KABLUKOVA[3], Vladimir KOMAROV[3], Ivan POPOV[1]

[1] *Институт Электронной Инженерии и Нанотехнологий им. Д.Гицу, АНМ*
[2] *Международная Лаборатория Сильных Магнитных Полей и Низких Температур, Вроцлав, Польша*
[3]*Herzen State Pedagogical University, ul. Kazanskaya (Plekhanova) 6, St. Petersburg, 191186 Russia*
**a.nikolaeva@nano.asm.md*

***Abstract* — We present the experimental results of an investigation of the electron transport of semimetal single- crystal $Bi_{1-x}Sb_x$ films and wires in temperature range 4.2-300 K. Bi-3at.%Sb films were prepared by the vacuum discrete thermal evaporation on a mica and polyimide substrates with different thickness. The individual 2at.% and 3at.%Sb wires with diameters from 100 nm to 1000 nm were prepared by the high frequency liquid phase casting. It was found that the appearance and increase of the energy gap ε_g in semimetal Bi–3 at.%Sb films with decreasing thickness correlates well with the value of ε_g in semimetallic Bi–2 at.%Sb wires and reaches the maximum value of 25–30 meV in the wires and films with d = 300 nm. The investigations of the Shubnikov de Haas oscillations on Bi-2at%Sb wires with d>600 nm show that overlapping of L and T bands was twice smaller than that in pure Bi. It is shown that the semimetal-semiconductor transition induced by the size quantization is observed in semimetal $Bi_{1-x}Sb_x$ films and wires occurs at diameters to five times greater than those in pure Bi. The compressive action of mica and tensile action of polyimide substrates allows manipulating the semimetal-semiconductor transition in quantum semimetalic $Bi_{1-x}Sb_x$ films.**

***Index Terms* — nanowires, films, semimetal-semiconductor transition, size quantization.**

**a.nikolaeva@nano.asm.md*

I. INTRODUCTION

Bismuth is a material where many new condensed matter phenomena were observed. This includes de Haas- van Alphen effect [1], quantum size confinement effect [2], quantum linear magnetoresistance [3], peculiar superconductivity [4], possibility fractional quantum Hall effect [5], oscillations Aaronov Bhom in quantum Bi wires [6].

Since the overlapping of L and T bands in semimetal $Bi_{1-x}Sb_x$ alloys is smaller than of those in pure Bi, the quantum confinement effects and in particular semimetal-semiconductor transition in $Bi_{1-x}Sb_x$ nanowires and films can be observed at much larger diameters than in pure Bi nanowires [7-8]. On the one hand, it simplifies the manufacturing technology of single-crystal quantum wires and films and application of methods to control their diameters. On the other hand, this will make it possible to separate the effects related to the size quantization and to the surface state, which were not taken into account in theoretical works [9-11] but play an important role in Bi wires with d~50 nm [12, 13].

A suitable material for studies of the influence of the quantum size effects on thermopower and resistance are single-crystal nanowires of $Bi_{1-x}Sb_x$ (0<x<0.04) in a glass capillary prepared by the high frequency liquid phase casting [14, 15, 16], and monocrystalline films prepared by thermal spraying on the mica substrate with subsequent recrystallisation under cover [17].

The goal of the present work is to reveal the critical phenomena which accompany the transition semimetal-semiconductor due to confinement effect in the $Bi_{1-x}Sb_x$ (x=0.02÷0.03) films and wires.

II. SAMPLES AND EXPERIMENT

Bismuth-antimony Bi-3at%Sb films were prepared by discrete thermal evaporation in vacuum (10-5 mm Hg.) on a substrate at the temperature of 410 K. Muscovite mica and a polyimide film were used as substrates. After deposition, the films were annealed at 540 K. The choice of material for substrates was mostly for two reasons. Mica has a crystalline structure, which has an orienting effect on a bismuth film and bismuth-antimony solid solutions, so that the orientation of crystallites of the films is usually characterized by the C_3 axis perpendicular to the substrate plane. A polyimide substrate is amorphous, but the film grows with the same orientation of the C_3 axis as it grows on a mica substrate.

To obtain monocrystalline bismuth and bismuth antimony films the method of zone recrystallization under cover was used [17].

The structure of the films was analyzed by the X-ray diffraction using the rotating crystal method in compliance with the Wolf-Bragg focusing (Fig. 1).

A small width of the diffraction peaks of the film as well as a good resolution of the X-ray peak of the doublet in the fifth order confirm the perfection of the crystal structure of the films and indicate a uniform distribution of antimony over the film.

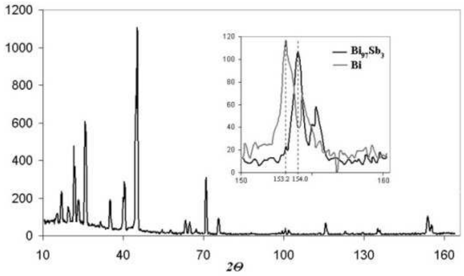

Fig. 1. X-ray diffraction pattern of Bi-3at%Sb film on mica. Inset: fifth-order peak of Bi and Bi-3at%Sb.

The etch pits are mirror images of the crystal orientation in the C_1C_2 basal plane and confirm that the film is single-crystal and (111) is oriented perpendicular to the film plane (Fig. 2).

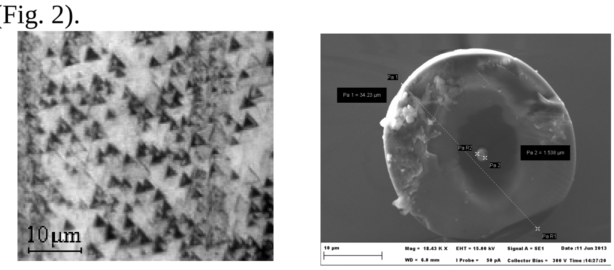

a) b)

Fig. 2. Optical microscopy image (a) of 50 μm single-crystal film after etching; SEM cross sectional image (b) of 1500 nm Bi-2at%Sb wire (clear) in glass envelope (gray).

Individual monocrystalline Bi-2at%Sb nanowires in a glass cover with different diameters were fabricated by the high frequency liquid phase casting (Ulitovsky- Taylor method) [16, 17].

Figure 2, b shows the SEM image of the $Bi_{1-x}Sb_x$ wire in a glass capillary. The wires had a strictly cylindrical shape. The glass envelope was very close to the wire surface and was more than an order of magnitude greater than the wire diameter.

The test measurements of the crystallographic orientation of the wires were carried out using an X calibur-E Diffractometer; they show that their principal axes are oriented along the (1011) crystallographic direction (Fig. 4, inset).

The investigation of the SdH oscillations in Bi and Bi-2%Sb wires was carried out in magnetic fields up to 14 T at liquid helium temperatures and at 1.5 K on a setup, which permitted automatic recording of the resistance R(H) and ∂R/∂H(H) curves at H||I and H⊥I.

Figure 3 shows the angular rotation diagrams transverse (ADTMR) (H⊥I) magnetoresistance the Bi-2at%Sb wires.

Using the ADTMR R(θ), (H⊥I), the wire was oriented in a magnetic field so, that the magnetic field vector $\vec{H}$ coincides with the certain crystallographic axes C_2 and C_3 of the wires Fig. 3).

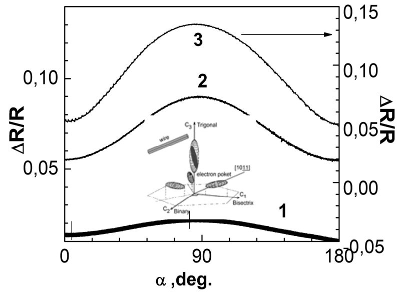

Fig. 3. Angular dependences of residual magnitoresistance in the trigonal-binary plane in constant magnetic field H=0.4 T (H⊥I), Bi-2at%Sb nanowires of different diameters: 1. d=300 nm; 2. d=600 nm; 3. d=900 nm, T=300 K. Inset: schematic diagrams of the Fermi surface electrons and holes relative to the main crystallographic direction and orientation of Bi wire.

Measurements in a strong magnetic field were performed in the International Laboratory of High Magnetic Fields and Low Temperatures (Wroclaw, Poland).

III. RESULTS AND DISCUSSION

The temperature dependences resistance R(T) films and wires with different diameters were measured in the temperature range 4.2- 300 K.

Figure 4 shows the temperature dependences of the resistivity R(T) of the Bi-3at%Sb films of two different thicknesses deposited on mica (a) and polyimide (b) substrates.

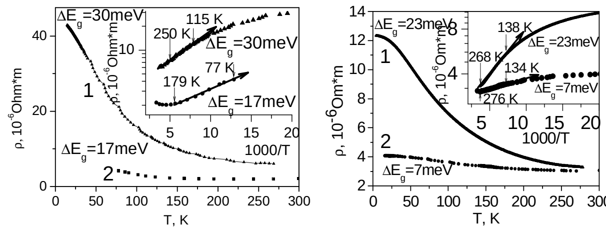

a) б)

Fig. 4. Experimental temperature dependences of resistivity ρ(T) of Bi-3at%Sb films, deposited on mica (a) and polyimide (b). Inset: dependences of $\rho(10^3/T)$ on thickness of film: 1. d=300 nm; 2. d=1000 nm.

Figures 4a and 4b (insets) show the dependences of the resistivity $\rho(10^3/T)$, which permits determination of the gap ε_g^{L}, T in films.

Figure 5 shows the temperature dependences of the residual resistance $\Delta R/R(T)=(R_T-R_0)/R_0(T)$ of Bi-2at%Sb wires with different diameters.

In the range of temperatures T>100 K on dependences $\rho(10^3/T)$ it is possible to allocate a linear curve pieces. On inclination of these pieces, according to the expression $\rho = \rho_0 exp\left(-\frac{\Delta E}{2\kappa T}\right)$, it was possible to calculate the energy gap width ε_g and its dependence on the diameter and a substrate kind.

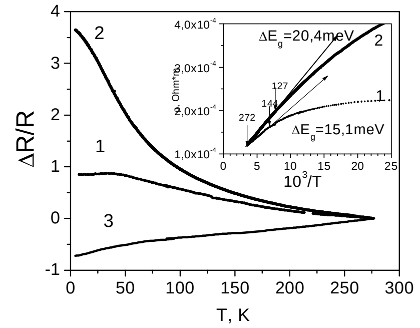

Fig. 5. Experimental temperature dependences of residual resistance ΔR/R(T) in Bi-2at%Sb wires: 1. d=200 nm; 2. d=500 nm; 3. d=1600 nm. Inset: dependences $\rho(10^3/T)$.

The maximum value of ε_g=30 meV for Bi-3at%Sb films (d=300 nm), deposited on mice and the minimum value of ε_g=7 meV for a Bi-3at%Sb deposited on polyimide were obtained.

On the one hand, it is because in Bi-3at%Sb films the overlapping of L and T bands ε_{ov} is less than in Bi-2at%Sb. On the other hand, the compressing action of mica and the stretching action of polyimide on the substrate lead to the maximal value of ε_g on the films deposited on mica and the minimal value of ε_g on the films with polyimide substrate.

For both films and wires the substantial temperature dependence of R (T) on the thickness was observed.

In Bi-2at%Sb wires the semimetal-semiconductor transition is observed at d<500 nm, while in the Bi-3at%Sb films the semiconductor dependence R(T) remain till the thickness becomes 1000nm (Figs. 4 a, b, curves 2). In Bi-2at%Sb wires with d=200 nm, the resistance R(T) increases 3.5 times.

In the temperature range of 4.2-300 K at Bi-3at%Sb films with the diameter of 300 nm deposited on mica the resistance R(T) increases 6-7 times (Fig. 4), and on a substrate from polyimide the resistance R(T) increases 3-4 times. Besides, unlike Bi-2at%Sb wires, the resistance R(T) 1000 nm of films on mica and polyimide substrate also increases 2.2 and 1.6 times, respectively.

On the one hand due to the fact that in the Bi-3at%Sb alloy the overlap T and L bands is less, compared with the Bi-2at%Sb and on the other hand in the deposited on the mica films observed of "compression" effect in the direction perpendicular to the film plane, which, also leads to a reduction of overlap of L and T bands, the highest value of the gap ε_g = 30 meV in Bi-3at%Sb films on the mica substrate (d = 300 nm) has been observed.

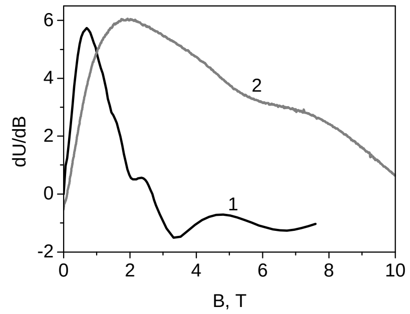

Fig. 6. SdH oscillation on Hall contacts in Bi films (d= 1000 nm) on mica substrate (1) and Bi-3%Sb on polyimide substrate (2), d= 300 nm.

This is confirmed by de Shubnikov de Haas (SdH) oscillations obtained on pure Bi films on mica- substrate (Fig. 6, curve 1) and films of Bi-3at.%Sb, obtained on polyimide (Fig. 6, curve 2).

Oscillatory dependences recorded in both the longitudinal (H||I), and the transverse magnetic fields (H||C_3 and H||C_2), which in each case allowed recovering the form of the electron and the hole Fermi surface in L and T points of the Brillouin zone.

For comparison, Fig. 7 shows the SdH oscillations in H||C_2 (H⊥I) direction of pure Bi (curve 1) and Bi-2at%Sb wires (curves 2, 3).

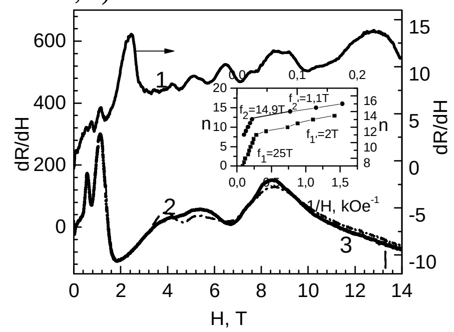

Fig. 7. SdH oscillation in Bi and Bi-2%Sb wires on derivative TMR $\partial\rho/\partial H(H)$, H⊥I, H||$C_2$. Inset: dependences of quantum number of SdH oscillations from inverse magnetic field 1/H. 1- pure Bi wire, 2 -T=4.2 K, 3 - T=2.1 K for Bi-2at%Sb, d=600 nm.

The SdH oscillations from both light electrons at L and holes at T in all Bi-2at%Sb wires with d> 300 nm were observed.

In this orientation, in a weak magnetic field, the oscillations from two equal mean main cross sections of the Fermi surface (FS) at L are observed. In strong magnetic fields, the oscillations from the maximum section S^T_{max} of holes in T have been observed. The regions of existence of the SdH oscillations from L electrons and T holes are separated in the magnetic field due to a significant difference in the extreme section FS of L electrons and T holes in this direction. Displacement of a field of a quantum limit of the SdH oscillations both from $L_{2,3}$ electrons and T holes in the area of a weak magnetic field is a clear evidence of a decrease of the Fermi surface in Bi-2at%Sb wires in comparison with those in pure Bi wires.

The frequency of the SdH oscillations $f_2=1/\Delta$ (H) from the maximum cross-section of the T hole ellipsoid decreases from 25 T to 14.9 T for pure Bi and Bi-2at%Sb wires. The frequency of the SdH oscillations from two equivalent electronic ellipsoids $L_{2,3}$ decreased almost 2-fold: from f_1=2 T to f_2=1,1 T.

The values of the Fermi level of the holes and electrons ε_F^h and ε_F^e were calculated according to expressions (1-3):

$$\varepsilon_F^T = \varepsilon_{par} - \frac{1}{2}\varepsilon_g^T + \left[\varepsilon_{par}^2 + \left(\frac{1}{2}\varepsilon_{gT}\right)^2\right]^{\frac{1}{2}} \qquad (1)$$

where ε_{par} is the energy in the parabolic band approximation, ε_F^T is holes of the Fermi energy (FE) in the

T point, m_c^T is the minimum cyclotron mass of T holes; ε_g^T = 200 meV is the gap in the T point of the Brillouin zone, Δ_T^{-1} - frequency of the SdH oscillations from the minimum cross section of the Fermi surface T- holes (S_T) at H||C_3, $\Delta_T\left(\frac{1}{H}\right)=\frac{2\pi e}{\hbar c S_T}$.

$$\varepsilon_{par}=\frac{S_T}{2\pi m_c^T}=\frac{eh\cdot\Delta_T^{-1}}{2\pi c\cdot m_c^T} \qquad (2)$$

The FL of the electrons in the L point is:

$$\varepsilon_F^e=\frac{eh}{2\pi}\times\frac{\Delta_e^{-1}}{m_c^e} \qquad (3)$$

Cyclotron masses of electrons and holes on the Fermi level were determined from the temperature dependence of the amplitude of the SdH oscillations at H||C_2 (Fig. 7, curves 2, 3).

It was establish, that the overlapping of L and T bands decreases up to E_{ov}=21 meV, which is almost twice less than in the pure Bi wires. So, really the semimetal-semiconductor transition in Bi-2at%Sb wires and films can occur at larger diameters than in pure Bi.

IV. CONCLUSION

It was found that the appearance and increase of the energy gap ε_g in semimetal Bi-3at%Sb films with decreasing thickness correlates well with the value of ε_g in semimetallic Bi-2at%Sb wires and reaches the maximum value of 25-30 meV in the wires and films with d=300 nm.

It is shown that the semimetal-semiconductor transition induced by the size quantization in single-crystal semimetal Bi1-xSbx films and wires occurs at diameters d, 5-7 times exceeding d in similar structures of pure Bi wires, which allows separating the effects related to the size quantization of the energy spectrum and those of the surface states.

The compressive action of mica and tensile action of polyimide substrates, along with thickness allows manipulating in the semimetal-semiconductor transition in quantum $Bi_{1-x}Sb_x$ films.

ACKNOWLEDGMENTS

This work was supported by the Moldo-Belarusian project 13.820.05.12/BF. The authors express their gratitude to Mr. Andrzej Karolewski from the International Laboratory of High Magnetic Fields and Low Temperatures for his assistance in the measurements at low temperatures in high magnetic fields.

REFERENCES

[1] W. J. de Haase and P. M. van Alphen. Proc. Acad. Sci. 33, 1106, (1930).
[2] Y. F. Ogrin, V. N. Lutskii, and M. I. Elinson. JETP Lett. 7, 71, (1966).
[3] A. A. Abrikosov. Europhus. Lett. 49, 789, (2000).
[4] W. Buckel and R. Hilsch, Z. Phys. 138, 109, (1654).
[5] K. Behnia, L. Balicas, and Y. Kopelevich. Science, 317, 1729, (2007).
[6] D. V. Gitsu, T. E. Huber, L. A. Konopko and A. A. Nikolaeva. Berry's phase manifestation in Aharonov-Bohm oscillations in single Bi nanowires. Journal of Physics: Conference Series, vol. 150, p. 022013, 2009.
[7] Yu-Ming Lin, O. Rabin, S. B. Cronin, Jackie Y. Ying and M. S. Dresselhaus. Semimetal–semiconductor transition in Bi1−xSbx alloy nanowires and their thermoelectric properties. Appl. Phys. Lett. 81, 2403 (2002).
[8] L. Hicks and M. S. Dresselhaus. Thermoelectric figure of merit of a one-dimensional conductor. Phys Rev B., 47, 16631, (1993).
[9] Y-M Lin, X. Sun, and M. S. Dresselhaus. Theoretical investigation of thermoelectric transport properties of cylindrical Bi nanowires. Phys Rev B., 62, 4610, (2000).
[10] M. S. Dresselhaus, G. Chen, M. Y. Tang, R. G. Yang, H. Lee, D. Wang, Z. Ren, J. P. Fleurial, and P. Gogna. New Directions for Low-Dimensional Thermoelectric Materials. Adv. Mater., 19, 1043, (2007).
[11] O. Rabin, Y.-M. Lin and M. S. Dresselhaus. Anomalously high thermoelectric figure of merit in Bi1-xSbx nanowires by carrier pocket alignment. Appl. Phys. Lett., 79, 81-83, (2001).
[12] Ph. Hofmann. The surfaces of bismuth: Structural and electronic properties. Prog. Surf. Sci., 81(5), 191, (2006).
[13] T. E. Huber, A. Adeyeye, A. Nikolaeva, L. Konopko, R. C. Johnos, and M. J. Graf. Surface state mobility and thermopower in semiconducting bismuth nanowires. Phys. Rev. B., 83, 2354114, (2011).
[14] N. B. Brand, D. V. Gitsu, A. A. Nikolaeva, and Ya. G. Ponomarev. Investigation of size effects in thin cylindrical bismuth single crystals in a magnetic field. JETP, 45(6), 1226, (1977).
[15] D. Gitsu, L. Konopko, A. Nikolaeva and T. Huber Pressure dependent thermopower of individual Bi nanowires. Appl. Phys. Lett., 86, 10210, (2005).
[16] A. Nikolaeva, T. E. Huber, D. Gitsu, and L. Konopko Diameter dependent thermopower of bismuth nanowires. Phys. Rev. B., 77, 035422, (2008).
[17] В. М. Грабов, В. А. Комаров, Е. В. Демидов, Н. С. Каблукова. Заявка на патент: Способ создания на различных подложках монокристаллических пленок многокомпонентного твердого раствора с равномерным распределением компонентов по объему. РФ пат. 2012128190/05, 2014. Бюл. №1.